

Real-time 100-GbE fiber-wireless seamless integration system using an electromagnetic dual-polarized single-input single-output wireless link at the W band

YUANCHENG CAI,^{1,2,*}  MIN ZHU,^{1,2,6}  JIAO ZHANG,^{1,2}  MINGZHENG LEI,²  BINGCHANG HUA,² YUCONG ZOU,² WEI LUO,¹ SHITONG XIANG,¹ LIANG TIAN,² JUNJIE DING,³  LIKE MA,⁴ YONGMING HUANG,^{1,2} JIANJUN YU,^{2,3} AND XIAOHU YOU^{1,2,5,7}

¹National Mobile Communications Research Laboratory, Southeast University, Nanjing 210096, China

²Purple Mountain Laboratories, Nanjing 211111, China

³Fudan University, 220 Handan Road, Shanghai 200433, China

⁴China Mobile Research Institute, Beijing 100053, China

⁵Peng Cheng Laboratory, Shenzhen 518000, China

⁶e-mail: minzhu@seu.edu.cn

⁷e-mail: xhyu@seu.edu.cn

*Corresponding author: caiyuancheng@pmlabs.com.cn

Received 21 November 2022; revised 10 January 2023; accepted 10 January 2023; posted 13 January 2023; published 7 February 2023

This Letter demonstrates a real-time 100-GbE fiber-wireless seamless integration system operating at the whole W band (75–110 GHz). Based on a pair of commercial digital coherent optical modules, the real-time transparent transmission of 125-Gb/s dual-polarized quadrature phase-shift keying signal has been successfully achieved over two-spans of 20-km fiber and up to 150-m electromagnetic dual-polarized single-input single-output wireless link. To the best of our knowledge, this is the first real-time demonstration of 100-GbE signal transmission over >100-m wireless distance at the millimeter-wave band based on photonics. We believed this real-time and high-speed fiber-wireless seamless integration system with a wireless coverage up to hundreds of meters can significantly accelerate the progress of upcoming 6G. © 2023 Optica Publishing Group

<https://doi.org/10.1364/OL.481386>

There is no doubt that millimeter-wave (MMW) and terahertz (THz) communications will play key roles in 6G networks, owing to their inherent large capacity and ultra-wideband characteristics [1,2]. However, some critical challenges remain at the current stage, which have become the major stumbling blocks for the application of high-frequency wireless communications. One is the restricted wireless coverage range, due to the high path loss of MMW/THz signals [3]. The other is the real-time process of high-speed (>100 Gb/s) and wideband (tens of gigahertz) MMW/THz signals in the wireless transceiver ends [4]. This is mainly limited by the bandwidth, sampling rate and resolution of existing analog-to-digital and digital-to-analog converters available for wireless communication systems. In addition, how to realize the transparent transmission and seamless integration

of large-capacity MMW/THz signals in the optical wireless networks is another issue worthy of concern.

Thanks to the advances in sophisticated optical coherence communication technology, the real-time processing of a high-speed optical baseband (BB) signal up to hundreds of GbE in commercial optical fiber communication systems has been realized with the aid of the mature digital coherent optical (DCO) modules. In previous research, the fiber-wireless-fiber (FWF) structure has been proposed to promote signal transparent transmission in hybrid optical fiber wireless channels [5–10]. Similarly, by adopting the mature DCO transceiver modules in the FWF system, the real-time emission and reception of high-speed wireless signal has been implemented [11,12], which is difficult or expensive for the traditional pure electronic wireless systems. Leveraging on the DCO-enabled FWF structure, we recently have successfully demonstrated an inspiring real-time 100-GbE signal delivery at the 0.33–0.5-THz band over hybrid fiber-THz-fiber transmission by using 2×2 multiple-input multiple-output (MIMO) THz wireless links [13,14]. However, due to the high air transmission loss as well as low optical-THz conversion efficiency, the wireless transmission distance is regrettably limited within the 10-m range. In addition, as shown in Fig. 1(a), when bridging an optical polarization division multiplexing (OPDM) signal, the two related components of the OPDM signal are transmitted over two separate branches of the 2×2 MIMO wireless channels. Hence, it is essential to precisely align and regulate the two sets of horn antennas (HAs) in actual implementation. It is because that the system performance of OPDM signal is susceptible to the mismatch of the beam direction, polarization state and link gain between the two separate wireless channels in this system. Moreover, the inter-channel interference and imbalance between the 2×2

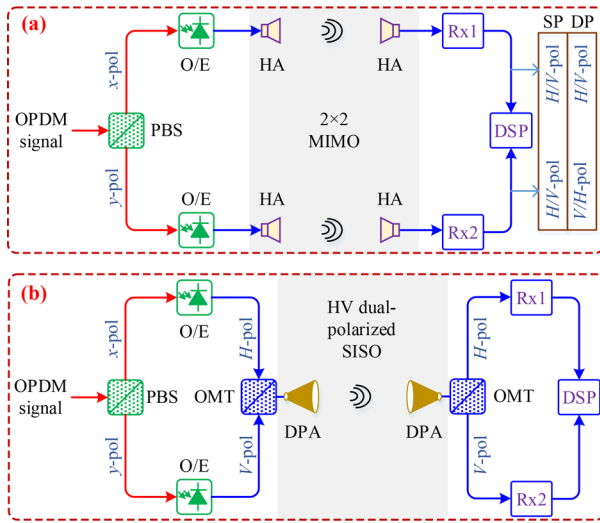


Fig. 1. Seamless integration for OPDM signal transmission by using (a) traditional 2×2 MIMO links and (b) a proposed electromagnetic dual-polarized SISO link with a pair of orthomode transducers (OMTs) and dual-polarized antennas (DPAs).

MIMO wireless links also lead to the performance degradation and instability.

To solve the above issues, as shown in Fig. 1(b), a dual-polarized single-input single-output (SISO) wireless link is adopted, which simultaneously transmits the horizontal and vertical polarization components of the W-band signal wave. Using a pair of orthomode transducers (OMTs) in conjunction with two dual-polarized antennas (DPAs), the OPDM signal can be skillfully coupled into an electromagnetic dual-polarized SISO wireless link, which significantly simplifies the traditional 2×2 MIMO links. As a result, the performance of the optical and wireless integration networks is further improved; meanwhile, this seamless integration scheme becomes more applicable and competitive. Based on the above-mentioned electromagnetic dual-polarized SISO wireless link and DCO-enabled FWF structure, we demonstrate a real-time fiber-wireless seamless integration system with W-band full spectrum communication in this Letter. A record real-time line rate of a 125-Gb/s dual-polarized quadrature phase-shift keying (DP-QPSK) signal has been delivered over up to 150-m wireless distance at the W band for the first time. Compared to our previous works, we not only simplify the wireless transmission link, but also extend more than 10 times the wireless distance, which are crucial for practical deployment of the upcoming high-speed 6G wireless communication. This paper is an extension of our work presented in [15]. The existing real-time demonstrations of fiber-wireless integration communication at the W band are also given in Table 1 as a contrast. Our demonstration system has significant advantages in both real-time communication rate and wireless transmission distance.

The experimental setup of the real-time 100-GbE DCO-enabled FWF seamless integration system over a W-band electromagnetic dual-polarized SISO link is shown in Fig. 2(a). Two identical optical transport units (OTUs), each equipped with a 100-GbE commercial DCO module, are used as the optical transmitter and receiver, respectively. The 100-GbE DCO module consists of one integrated coherent transmitting (ICT) and one integrated coherent receiving (ICR) unit, which can

Table 1. Summary of Real-Time Demonstrations of Fiber-Wireless Integration Communication at the W-band

Year	Frequency/GHz	Line Rate/Gb/s	Distance/m	Ref.
2013	81.6	1.25	5	[16]
2014	87.6	1.25	1	[17]
2017	83	2.5	50	[18]
2017	91	24.08	3	[19]
2018	96	5.0	20	[20]
2018	79.3	16.69	1	[21]
2022	92.5	125.516	150	This work

realize the real-time emission and reception of a 31.379-GBd optical DP-QPSK BB signal, respectively. With a rolloff of 0.2, the real-time OPDM output signal has a whole bandwidth of approximately 37.65 GHz. Its center wavelength is approximately 1549.315 nm with a launch power of 3 dBm. After 20-km standard single-mode fiber (SSMF) transmission, the optical DP-QPSK BB signal is amplified by an erbium-doped fiber amplifier (EDFA1), and the corresponding out-of-band amplified spontaneous emission (ASE) noise is suppressed via a tunable optical filter (TOF1).

At the optical-wireless conversion module, the photonics-aided method is used to generate the desired MMW signal. An external cavity laser (ECL1) with the wavelength of 1550.056 nm and power of 10 dBm is served as optical local oscillator (LO). After adjusting the appropriate polarization directions by two polarization controllers (PCs), the LO and signal lightwaves are coupled together by a polarization-maintaining optical coupler (PMOC). The frequency difference between the two lightwaves is 92.5 GHz, whose optical spectrum is given in Fig. 3(a). Two orthogonal optical polarization components, i.e., X and Y polarizations, are separated by a polarization beam splitter (PBS), and then converted to a 92.5-GHz MMW signal via two identical photodiodes (i.e., PD1 and PD2) with a 3-dB bandwidth of 100 GHz and responsivity of 0.6 A/W. A variable optical attenuator (VOA1) is placed before the PBS to adjust the input power into the two PDs. Note that the obtained MMW signal occupies the whole spectrum of the W band (75–110 GHz) with a total bandwidth of 37.65 GHz. Afterward, the two related MMW components are amplified by two identical low noise amplifiers (LNA1 and LNA2) with the gain of 35 dB, respectively. Then one W-band OMT (i.e., OMT1) with 35-dB isolation between the horizontal polarization (H-pol) and vertical polarization (V-pol) is used to combine the two components together. Thereby, a 125-Gb/s HV dual-polarized MMW signal at 92.5 GHz can be obtained. Subsequently, a pair of DPAs, herein, the lens corrected antennas (LCAs) with total gain of 2×30 dBi are used to establish a W-band electromagnetic dual-polarized SISO wireless link, which can avoid the inter-channel interference and imbalance incurred from the 2×2 MIMO channels in our previous work [13]. A wireless delivery distance up to 150 m is achieved in this experiment. To enhance the MMW receiving power, a home-made polytetrafluoroethylene lens with a diameter of 30 cm and a focal length of 50 cm, which can provide approximately 50-dBi gain [22], is placed before the receiving antenna (i.e., LCA2) to focus the divergent MMW beam due to long-distance transmission. The photos of the outdoor W-band emission end, 150-m wireless transmission link, and indoor reception end are also given as Figs. 2(b) and 2(c), respectively.

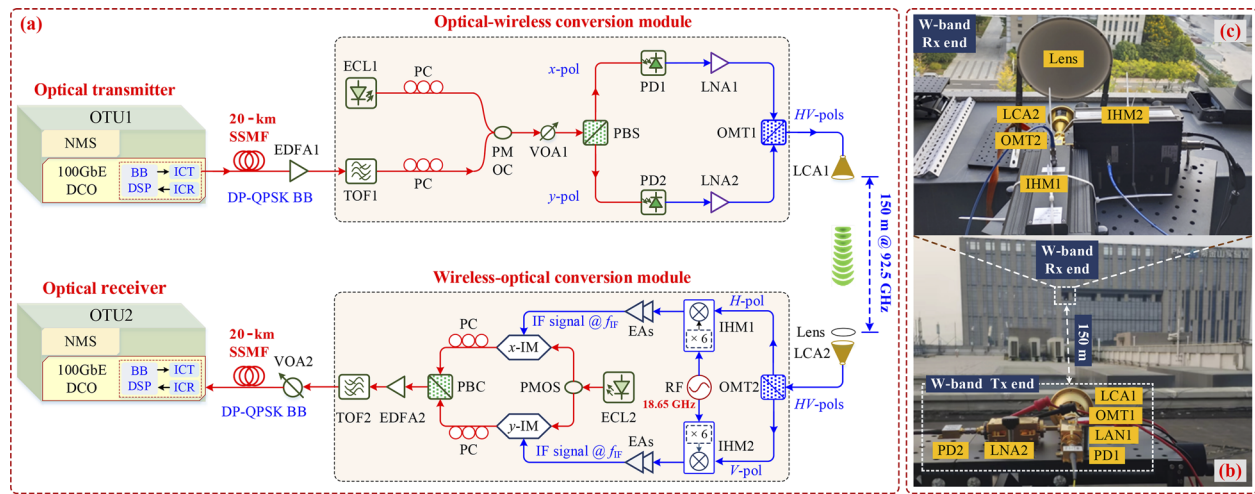


Fig. 2. (a) Experimental setup of real-time 100-GbE DCO-enabled FWF seamless integration system over a W-band electromagnetic dual-polarized SISO link. Photos of (b) outdoor W-band emission end, transmission link, and (c) indoor W-band reception end.

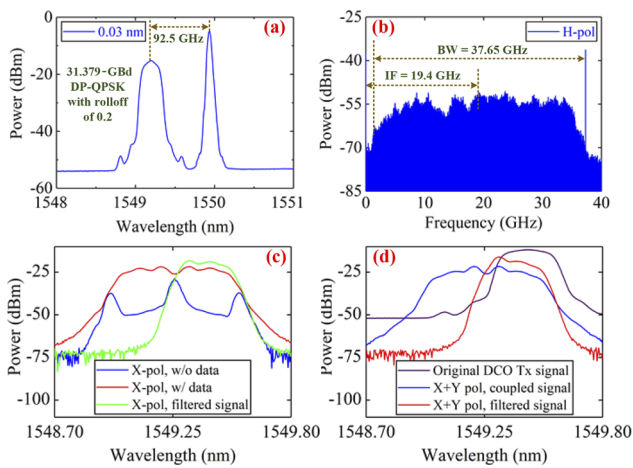


Fig. 3. (a) Optical spectrum after OC. (b) Electrical spectrum of H-polarization IF signal after downconversion. (c) Optical spectra of X-polarization with and without a 31.379-GbD QPSK signal and (d) coupled PDM signal before and after TOF2.

To realize the real-time optical reception of the 100-GbE signal, the signal transparent conversion from the MMW band to optical BB is necessary at the wireless-optical conversion module. This can be conducted via the following two steps. One is electronic downconversion from the MMW band to intermediate frequency (IF) signal. The other is electro-optic re-modulation and filtering to produce the desired optical BB from the obtained electrical IF signal. As shown in Fig. 2(a), the received *HV* dual-polarized MMW signal is first re-split into two orthogonal electromagnetic polarizations (i.e., *H-pol* and *V-pol*) via the OMT2. Then two identical W-band integrated harmonic mixers (IHMs), which consist of a sixfold frequency multiplier chain and a mixer, are used to achieve the MMW frequency down-conversion. The input RF source is set to 18.65 GHz with the power of 7 dBm. Accordingly, each downconverted IF signal has a center frequency of 19.4 GHz and the whole bandwidth of 37.65 GHz, as shown in Fig. 3(b). Then, the above two IF signals are separately amplified by two identical sets of cascaded electrical amplifiers (EAs) with a 3-dB bandwidth of

47 GHz. They are subsequently fed to two independent intensity modulators (IMs) with 3-dB bandwidths of 40 GHz. A second ECL (ECL2) with the center wavelength of 1549.124 nm and power of 14.5 dBm serves as the input optical carrier of the two IMs. This optical carrier, which has a 23.8-GHz frequency spacing to the original optical DP-QPSK BB signal, is split evenly by a polarization-maintaining optical splitter (PMOS) into two branches. With biasing each IM at its null point, the carrier-suppressed double-sideband (CS-DSB) modulation can be realized in both branches. Subsequently, the two CS-DSB components are coupled again by one polarization beam coupler (PBC) with appropriate polarization control through two PCs. The generated dual-polarized CS-DSB signal is first boosted by the EDFA2, and then is fed to a second TOF (i.e., TOF2). By filtering out the lower sideband and undesired ASE noise, an optical DP-QPSK BB signal which is conveyed by the upper sideband with the center wavelength of 1549.279 nm can be successfully obtained. Figures 3(c) and 3(d) show the corresponding optical spectra of X-polarization with and without a 31.379-GbD QPSK signal and coupled PDM signal before and after TOF2, respectively. Noting that a small frequency spacing between the filtered optical DP-QPSK BB signal and original DCO Tx signal can be seen from Fig. 3(d), it is a result after optimization according to the best bit error ratio (BER) performance.

At the optical receiver end, after transmitting over another span of 20-km SSMF, the above-obtained optical DP-QPSK BB signal is fed to the 100-GbE DCO of OTU2 for real-time reception and demodulation. The optical signal-to-noise ratio (OSNR) and BER can be monitored in real time by the ICR unit of the DCO module and intuitively displayed through an embedded network management system (NMS) operation interface in OTU2 [14].

To evaluate the transmission performance of this system, we first study the OSNR and BER curves versus different input optical power into each PD under two spans of 20-km SSMF and 100-/150-m wireless links, as shown in Figs. 4(a) and 4(b). As can be seen from Fig. 4(a), the optimal input optical power for optical-MMW conversion is 6 dBm. A larger power degrades the system performance due to the saturation effect of the PD. Under the optimal input optical power, the OSNRs for 100-m and 150-m wireless transmission are 14.2 dB and 13.3 dB,

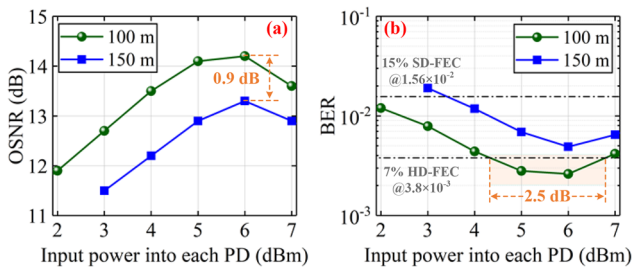


Fig. 4. (a) OSNR and (b) BER versus input optical power into each PD for the real-time transmission of a 125-Gb/s DP-QPSK signal.

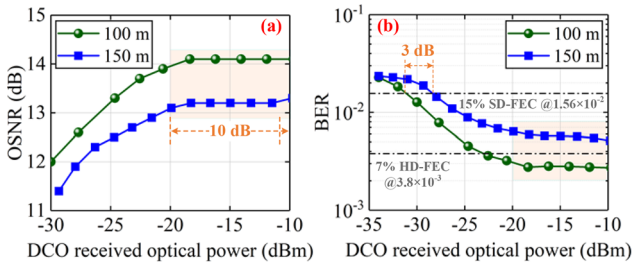


Fig. 5. (a) OSNR and (b) BER versus DCO received optical power for the real-time transmission of a 125-Gb/s DP-QPSK signal.

respectively, which exhibits a penalty of only 0.9 dB. For both of the above two cases, an optical power greater than 3.5 dBm can reach the BER threshold (1.56×10^{-2}) of 15% overhead soft-decision (SD) forward-error-correction (FEC), as shown in Fig. 4(b). In particular, the BER of 100-m case can even reach 7% overhead hard-decision (HD) FEC threshold (3.8×10^{-3}) with a power margin of 2.5-dB from 4 dBm to 7 dBm. Therefore, after excluding the FEC overhead, the real-time transmission net rates of a 31.379-GBd DP-QPSK signal for the 100-m and 150-m cases are 117.30 Gb/s and 109.14 Gb/s, respectively.

Under the same FWF link with an optimal optical power of 6 dBm for optical-MMW conversion, we further investigate the OSNR and BER performance with different DCO received optical power (ROP), as shown in Figs. 5(a) and 5(b). Both the OSNR and BER curves have a stable region for 100-m and 150-m cases, where an appreciable receiving sensitivity margin of over 10 dB can be observed. In addition, under the 15% overhead SD-FEC threshold, the receiving sensitivity of the 100-m and 150-m cases are approximately -31.3 dBm and -28.1 dBm, respectively. Thus, the power penalty caused by an additional 50-m wireless transmission is approximately 3.2 dB, which is roughly in accordance with the theoretical prediction of 3.5 dB. By analogy, the 125-Gb/s DP-QPSK signal could be transported approximately 300 m (i.e., $150 \text{ m} + 50 \text{ m} \times (-19 - (-28))/3$) in this system before reaching the 15% overhead SD-FEC threshold using -19 dBm as a reference. Such a long-reach wireless transmission distance can well meet the needs of future 6G high-speed wireless access networks, which are composed of multiple macro stations and the wireless coverage range of each station is just within 300 m.

In conclusion, a real-time 125-Gb/s DP-QPSK signal transmission over two spans of 20-km SSMF and up to 150-m wireless at the W band has been demonstrated for the first time. Based on the DCO-enabled FWF structure, we have successfully achieved a record real-time net rates of 117.30 Gb/s for

100 m and 109.14 Gb/s for 150 m by using a simplified W-band electromagnetic dual-polarized SISO link. This real-time 100-GbE fiber-wireless seamless integration system with the long-distance wireless transmission can provide a promising solution for the future MMW-enabled 6G networks.

Funding. National Natural Science Foundation of China (62101126, 62101121, 62201393, 62201397, 62271135); Natural Science Foundation of Jiangsu Province (BK20221194).

Disclosures. The authors declare no conflicts of interest.

Data availability. Data underlying the results presented in this paper are not publicly available at this time but may be obtained from the authors upon reasonable request.

REFERENCES

- X. You, C. X. Wang, and J. Huang, *et al.*, *Sci. China Inf. Sci.* **64**, 110301 (2021).
- I. Akyildiz, A. Kak, and S. Nie, *IEEE Access* **8**, 133995 (2020).
- T. Nagatsuma, G. Ducournau, and C. C. Renaud, *Nat. Photonics* **10**, 371 (2016).
- I. F. Akyildiz, C. Han, Z. Hu, S. Nie, and J. M. Jornet, *IEEE Trans. Commun.* **70**, 4250 (2022).
- Y. Salamin, B. Baeuerle, W. Heni, F. C. Abrecht, A. Josten, Y. Fedoryshyn, C. Haffner, R. Bonjour, T. Watanabe, M. Burla, D. L. Elder, L. R. Dalton, and J. Leuthold, *Nat. Photonics* **12**, 749 (2018).
- T. Kawanishi, *J. Lightwave Technol.* **37**, 1671 (2019).
- P. T. Dat, T. Umezawa, A. Kanno, N. Yamamoto, and T. Kawanishi, *Opt. Lett.* **47**, 1149 (2022).
- M. Zhu, J. Zhang, B. Hua, M. Lei, Y. Cai, L. Tian, D. Wang, W. Xu, C. Zhang, Y. Huang, J. Yu, and X. You, *Sci. China Inf. Sci.* **66**, 113301 (2023).
- Y. Horst, T. Blatter, L. Kulmer, B. I. Bitachon, B. Baeuerle, M. Destraz, W. Heni, S. Koepfli, P. Habegger, M. Eppenberger, E. De Leo, C. Hoessbacher, D. L. Elder, S. R. Hammond, L. E. Johnson, L. R. Dalton, Y. Fedoryshyn, Y. Salamin, M. Burla, and J. Leuthold, *J. Lightwave Technol.* **40**, 1690 (2022).
- X. Li, J. Yu, J. Xiao, and Y. Xu, *IEEE Photonics Technol. Lett.* **26**, 1948 (2014).
- C. Castro, R. Elschner, T. Merkle, C. Schubert, and R. Freund, *Optical Fiber Communication Conference (OFC)* (2020), paper M4I.2.
- C. Wang, X. Li, M. Zhao, K. Wang, J. Zhang, M. Kong, W. Zhou, J. Xiao, and J. Yu, *Optical Fiber Communication Conference (OFC)* (2020), paper W2A.42.
- J. Zhang, M. Zhu, M. Lei, B. Hua, Y. Cai, Y. Zou, L. Tian, A. Li, Y. Wang, Y. Huang, J. Yu, and X. You, *Opt. Lett.* **47**, 1214 (2022).
- J. Zhang, M. Zhu, B. Hua, M. Lei, Y. Cai, Y. Zou, W. Tong, J. Ding, L. Tian, L. Ma, J. Xiao, Y. Huang, J. Yu, and X. You, *J. Lightwave Technol.* **41**, 1129 (2023).
- Y. Cai, M. Zhu, J. Zhang, M. Lei, B. Hua, Y. Zou, W. Luo, S. Xiang, L. Tian, J. Ding, L. Ma, Y. Huang, J. Yu, and X. You, in *Optical Fiber Communication Conference (OFC)* (2023), paper Tu3J.1.
- J. J. Vegas Olmos, X. Pang, A. Lebedev, and I. T. Monroy, in *Asia Communications and Photonics Conference (ACP)* (2013), AT3G.1.
- X. Pand, A. Lebedev, J. J. Vegas Olmos, and I. T. Monroy, *J. Lightwave Technol.* **32**, 4585 (2014).
- L. Chorchos, S. Rommel, J. P. Turkiewicz, I. Tafur Monroy, and J. J. Vegas Olmos, *IEEE Photonics Technol. Lett.* **29**, 489 (2017).
- X. Li, X. Xiao, Y. Xu, K. Wang, L. Zhao, J. Xiao, and J. Yu, in *2017 Optical Fiber Communications Conference and Exhibition (OFC)* (2017), paper M3E.3.
- A. Bekkali, T. Kobayashi, K. Nishimura, N. Shibagaki, K. Kashima, and Y. Sato, *J. Lightwave Technol.* **36**, 3988 (2018).
- R. Deng, J. Yu, J. He, M. Chen, Y. Wei, L. Zhao, Q. Zhang, and X. Xin, *J. Lightwave Technol.* **36**, 5562 (2018).
- W. Li, J. Yu, J. Ding, Y. Tan, Y. Wang, J. Zhang, C. Wang, L. Zhao, K. Wang, W. Zhou, M. Zhu, and J. Yu, *IEEE Photonics Technol. Lett.* **34**, 858 (2022).